THE PENNSYLVANIA STATE UNIVERSITY
SCHREYER HONORS COLLEGE

SCHOOL OF SCIENCE

CHARACTERIZING AND OPTIMIZING THE SYNTHESIS OF 'BUBBLE' DNA-TEMPLATED SILVER NANOCLUSTERS AS A FLUORESCENT MATERIAL

IAN E. CAMPBELL
SPRING 2016

A thesis
submitted in partial fulfillment
of the requirements
for a baccalaureate degree
in Chemistry
with interdisciplinary honors in Chemistry and Physics

Reviewed and approved* by the following:

Bruce Wittmershaus
Associate Professor of Physics
Thesis Supervisor

Alan Jircitano
Associate Professor of Chemistry
Honors Adviser

Darren Williams
Professor of Physics and Astronomy
Thesis Reader

* Signatures are on file in the Schreyer Honors College.

ABSTRACT

A new format of DNA-templated silver nanoclusters (AgNCs) has been synthesized by hybridizing the strands 5'- CTGACTCCC*n*TGGGAGAA -3' and 5'- TTCTCCCAC*n*GGAGTCAG -3' with *n*=2, 3, 4, 5, 6, 7, 8, 10, 12, and 16 cytosine pairs in water and phosphate buffer (pH=7). Fluorescent populations emitting at ~545nm and ~630nm and absorbing at ~470nm and ~570nm, respectively, were formed from each bubble template. The bubble template with 8 cytosine pairs formed the brightest ~630nm emitter, while the 7 cytosine pair template formed the brightest ~545nm emitter. The template with 8 cytosine pairs formed the most stable AgNCs with the ~545nm emission increasing over the course of 116 hours and the ~630nm emission reaching ~16% its maximum value after 116 hours. Preliminary optimized Ag:$NaBH_4$:DNA was found to be 14:14:1. Single stranded bubble templates were found to be much less stable than hybridized bubble templates. Finally, optimal phosphate buffer (pH=7) concentration, DNA concentration, silver-to-DNA ratio, and silver-to-sodium borohydride ratio were found to be 7.88μM, 10μM, 11.25, and 2.20, respectively, via Box-Behnken experimental design with chemical yield and photostability as response factors.

TABLE OF CONTENTS

LIST OF FIGURES

LIST OF TABLES

ACKNOWLEDGEMENTS

I would like to than Dr. Wittmershaus for his consistent support and leadership. I would also like to thank Robert Passerotti, Nicholas Swanson, and Danielle Stanko for assisting me with this research. I thank the Biology and Chemistry Departments at Penn State Behrend for their consultation and consent in using their instruments. Finally, I am extremely grateful to the Erikson Discovery Grant for providing essential funds that allowed me to perform as a student researcher.

This material is also based upon work supported by the National Science Foundation under Grant Number NSF-ECCS-1306157.

Chapter 1

Introduction

Luminescent solar concentrators (LSCs) are sheets of clear plastic or glass that contain or are coated with fluorophores (Figure 1). Sunlight incident on the top of an LSC enters the sheet, is absorbed by the fluorophores, and then reemitted within the sheet. Since the LSC's index of refraction is higher than that of its surroundings, fluorescence at an angle beyond the critical angle of the LSC material is trapped within the sheet by a process known as total internal reflection. Up to 74% of the fluorescence is then reflected between the two internal surfaces of the LSC until it reaches the edges where semiconductor photovoltaic cells (PVCs) convert it to electrical energy. [1]

LSCs are not energy converting devices, like PVCs, but they can be used to reduce the amount of expensive PVC material needed by collecting light over a large area and concentrating it. A LSC-PVC system is less efficient per area than regular solar cells, but this combination has the potential for being so inexpensive that its low cost outweighs its inefficiency. Unfortunately, the fluorophores presently used in LSCs (quantum dots, phosphors, organic dyes) are either too expensive or too unstable for a long-term light-concentrating device.

Our laboratory recently found literature describing the synthesis and characterization of fluorescent DNA-templated silver nanoclusters (DNA-AgNCs), which were first prepared in 1998. [2] DNA-AgNCs are generally prepared by dissolving silver salts in purified water containing DNA. The positively charged silver ions are attracted to the negative nitrogenous bases of DNA via electrostatic interactions. A reducing agent is added and donates

one electron per silver ion yielding neutral clusters of silver atoms. Reducing lone silver ions in water results in bulk metal due to excessive aggregation, however including a DNA template in the reaction mediates the atoms' reactivity and creates nanoclusters of 2-20 atoms. Nanoclusters behave differently than bulk silver metal and quantum mechanical effects, like surface plasmon resonance, allow the cluster to absorb and fluoresce light at wavelengths in the visible region.

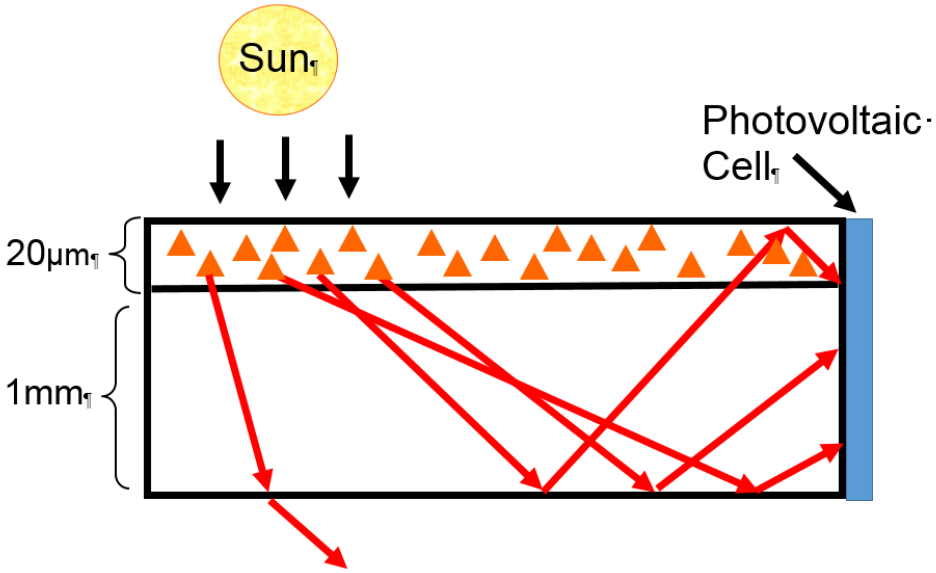

Figure 1. Schematic of an operating thin film LSC.

Solar energy incident upon the LSC is absorbed by the fluorophores in the 20μm film layered upon a 1mm high-index glass sheet. Fluorescence is guided to the PVC on the thin edge by total internal reflection.

Most literature examples describe AgNC formation on single-stranded DNA (ssDNA) that bends into hairpin formations (Figure 2). ssDNA-AgNCs have not been subjected to many stability studies, and only a few strands have been shown to yield long-lived fluorescent clusters. [3] Different sequences of ssDNA templates each give rise to cluster populations of distinct

absorption and emission energies. Reproducibility and common procedures are also scant in the literature as no DNA-AgNC studies have reported the details of systematically varied reaction conditions. Due to DNA-AgNCs' sensitivity to reaction conditions, they show potential for large improvements in the way of chemical yield, photo and chemical stabilities, and fluorescence quantum yield. If such improvements were realized, it could result in their use as a fluorescent material for LSCs. I propose that a single template design can also yield differently colored clusters with subtle, controlled modifications.

My peers and I devised the first double-stranded DNA (dsDNA) template for AgNCs. It consists of a "bubble" of identical cytosine bases inspired by Orbach's nanowires (Figure 2). [4] DNA bubbles are made of two DNA strands with eight complementary bases on either side of a sequence of *n* cytosine bases (Figure 2). My research shows that bubble DNA templates form stable, highly fluorescent AgNCs. I document that they can be prepared by a well-established and extensively documented procedure.

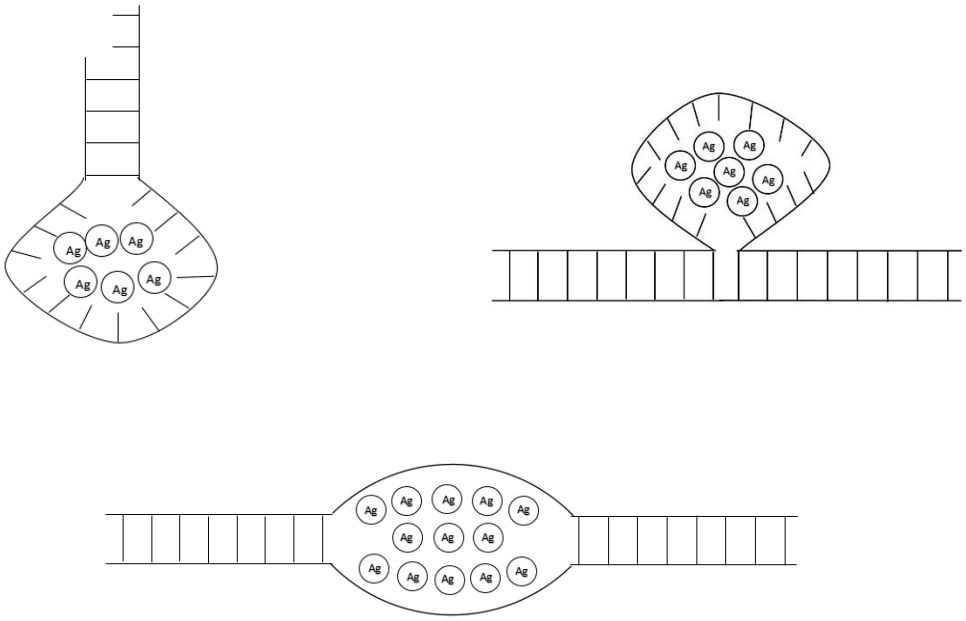

Figure 2. Cartoon representations of different DNA templates.

Top left, top right, and bottom depict a hairpin, nanowire, and bubble, respectively. Note that the wire is formed by repeating units.

Four general experiment paths are explored in my thesis. The first determined which value of *n* cytosine bases created AgNCs most suited for energy collection, i.e. the most absorbing, strongly emitting, and most photostable. The second examined the optimal silver-to-sodium borohydride-to-DNA ratio to gain a sense of optimal synthesis parameters. Third, AgNCs were made using the ssDNA template from the optimal bubble size to determine whether hybridization stabilized the AgNCs. Finally, optimization for the new procedure for synthesizing bubble DNA-AgNCs was determined using a Box-Behnken experimental design [5], which

considers response factors, or dependent variables, as functions of multiple control factors, or independent variables (Figure 3). Effects of control factors on response factors must be quantifiable so they can be analyzed in multiple-dimensional space where all control factors act as parameters. Herein, is reported the first preparation of dsDNA AgNCs and the optimization of their synthesis procedure with respect to DNA concentration, buffer concentration, silver-to-DNA ratio, and reducing agent-to-silver ratio.

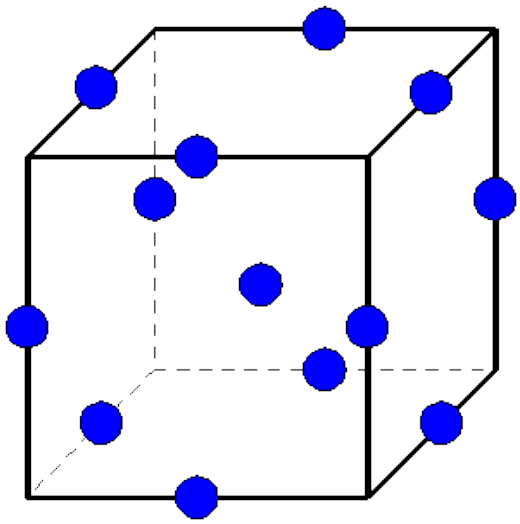

Figure 3. A pictorial representation of a Box-Behnken experimental design

The cube represents an experiment manipulated with respect to three variables (i.e. in three dimensions). Each point corresponds to a combination of the three control factors at different numerical values. Response factors are observed at each point to plot how they are affected over each control factor's range; graphically representing this change gives a response surface. The point directly in the center is known as a center point and represents the middle of the range of each control factor. This report discusses a four-dimensional design. Image credit: Engineering Statistics Handbook of the National Institute of Standards and Technology (NIST) [6].

Chapter 2
Materials and Methods

2.1 Common Materials

All DNA samples were customized sequences purchased from Integrated DNA Technologies (IDT). DNA bubbles were compose of sequences 5'-CTGACTCCC*n*TGGGAGAA -3' and 5'- TTCTCCCAC*n*GGAGTCAG -3', which were named B*n*C Top and B*n*C Bottom, respectively, where *n* is equal to the number of cytosine bases in each strand. Only B*n*C Top and Bottom strands of equal *n* were paired. Solid silver nitrate (≥99.0% $AgNO_3$) and sodium borohydride (≥98.0% $NaBH_4$) were purchased form Sigma Aldrich. All AgNC solutions were prepared in 1.5mL Eppendorf tubes containing water (18MΩ) purified by reverse osmosis. All $AgNO_3$ stock solutions were stored in a dark refrigerator at 5 ^{0}C and all $NaBH_4$ solutions were prepared within 30 seconds of use. For spectroscopic analyses, solutions were placed into disposable, acrylic 0.3 x 1.0 cm cuvettes (FireflySci).

2.2 Optimizing *n* in B*n*C Bubble DNA Templates

Bubble DNA templates were synthesized using ssDNA strands with *n*= 2, 3, 4, 5, 6, 7, 8, 10, 12, and 16 cytosine pairs. Each strand was dissolved in enough purified water to make 200μM solutions of Top and Bottom strands. Equal volumes of these solutions were mixed and annealed to 85˚C for 15 minutes, then cooled overnight in Styrofoam to make a 100μM solution of hybridized bubble DNA. 0.5 mL of the bubble solution was diluted to 25μM with water. The

DNA:Ag:$NaBH_4$ ratio used in preparing the clusters is 1:6:6. A dsDNA bubble template was counted as one unit of DNA in this ratio. 20µL of cold 0.015M $AgNO_3$ solution was added to the bubble solution, which was subsequently mixed by a vortex mixer for 2 minutes and chilled in an ice-water bath for 18 minutes. Meanwhile, an aqueous 0.03M $NaBH_4$ solution was prepared in cold water with solid $NaBH_4$. 10µL of 0.03M $NaBH_4$ solution was added to the bubble DNA-Ag solution. It was then vortexed for 2 minutes, chilled for 28 minutes, and allowed to warm to room temperature before spectroscopic measurements were taken. Time t=0 occurred once the bubble DNA-AgNC solution was withdrawn from the ice. The final bubble DNA AgNC solutions were stored in the dark at room temperature in between spectroscopic measurements.

2.3 Optimizing Silver-to-Sodium Borohydride-to-DNA Ratio for B8C AgNCs

Before carrying out the more extensive Box-Behnken experimental design [6], more limited experiments were carried out to determine the best silver-to-sodium borohydride-to-DNA ratio. B8C and B12C bubbles' fluorescence properties were tested at Ag:$NaBH_4$:DNA ratios of 24:24:1, 20:20:1, 18:18:1, 16:16:1, 14:14:1, 12:12:1, 10:10:1, 8:8:1, 6:6:1, 4:4:1, and 2:2:1. A 100µM hybridized bubble DNA solution was prepared as described in Procedures for Optimizing *n* in B8C bubble DNA Templates (section 2.2). This solution was diluted to 50µM and 100µL of it was placed into each of 11 different, non-adjacent wells in a 96-well microtitre plate. The 0.015M $AgNO_3$ solution was diluted to 0.00375M, which was used with equal volumes of a 0.00375M $NaBH_4$ solution to react with different bubble DNA samples at different Ag:$NaBH_4$:DNA ratios. Each well was diluted to a final volume of 200µL to ensure uniform

optical effects. The fluorescence of each of these samples was characterized with a Kodak Image Station 4000R Pro and Carestream Molecular Imaging Software.

2.4 Comparing Single and Hybridized B8C Bubble DNA Sequences

B8C Top and Bottom strands were prepared as described in Procedures for Optimizing n in BnC Bubble DNA Templates (section 2.2) except they were never hybridized.

2.5 Synthesis Optimization Via a Box-Behnken Experimental Design

A Box-Behnken experimental design [6] was established considering AgNC chemical yield, photostability, and fluorescence quantum yield as response factors and phosphate buffer (pH=7) concentration, DNA concentration, silver-to-DNA ratio, and silver-to-sodium borohydride ratio as control factors. The design consisted of 27 experiments using different combinations of the four control factors as seen in Appendix A. Each control factor was assigned three points: one on either end of a chosen range and one in the center of this range.

All solutions and diluents were chilled in an ice-water bath and stored in a dark refrigerator at 5 ^{0}C. These experiments were performed by dissolving solid B8C Top and Bottom DNA in purified water to give 1mM solutions. These solutions were mixed at equal volumes, annealed to 94˚C for 15 minutes, and then cooled overnight in Styrofoam, forming a 500μM solution of bubble DNA. 500μM of bubble DNA was diluted with purified water and 0.2M phosphate buffer (pH=7) to the appropriate concentration of buffer, then mixed with 10μL $AgNO_3$ at various concentrations diluted from a 0.2M stock solution. The solutions were vortexed and chilled in an ice-water bath for 2 and 18 minutes, respectively. Finally, solid

$NaBH_4$ was dissolved in purified water and shaken in a tinted bottle for exactly 30 seconds to mix. The silver-DNA solution was mixed with the desired amount of $NaBH_4$ solution for 2 minutes by vortexing and then chilled for 28 minutes. Time t=0 occurred when the solutions were removed from the ice-water bath. The final B8C AgNC solutions were stored in the dark at room temperature in between spectroscopic measurements.

These B8C AgNCs' fluorescence intensities were monitored as a function of time, yielding data that was processed using Minitab 16 Statistical Software to give response surfaces showing response factors' dependencies on control factors.

Chapter 3

Results

3.1 Optimizing *n* in B*n*C Bubble DNA Templates

Bubble DNA templates with *n*=2,3,4,5,6,7,8,10,12, and 16 cytosine pairs were synthesized and used to form AgNCs. Figures 4, 5, and 6 show absorption and adjusted fluorescence spectra of B5C, B7C, and B8C AgNCs 2 hours after synthesis, respectively. Fluorescence spectra in figures 4, 5, and 6 have been divided by their corresponding absorbance values at the excitation wavelength, so that relative fluorescence intensities can be compared.

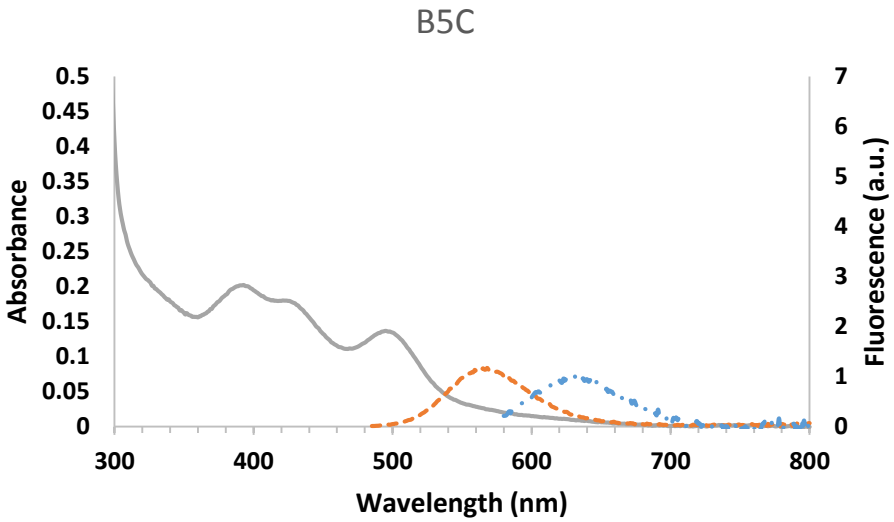

Figure 4. Absorbance and fluorescence spectra at excitation wavelengths of 465nm and 560nm from B5C AgNCs at 2 hours after synthesis

The grey solid line corresponds to the absorbance spectrum and the orange dashed and blue alternating lines correspond to fluorescence spectra at excitation wavelengths of 465nm and 560nm, respectively.

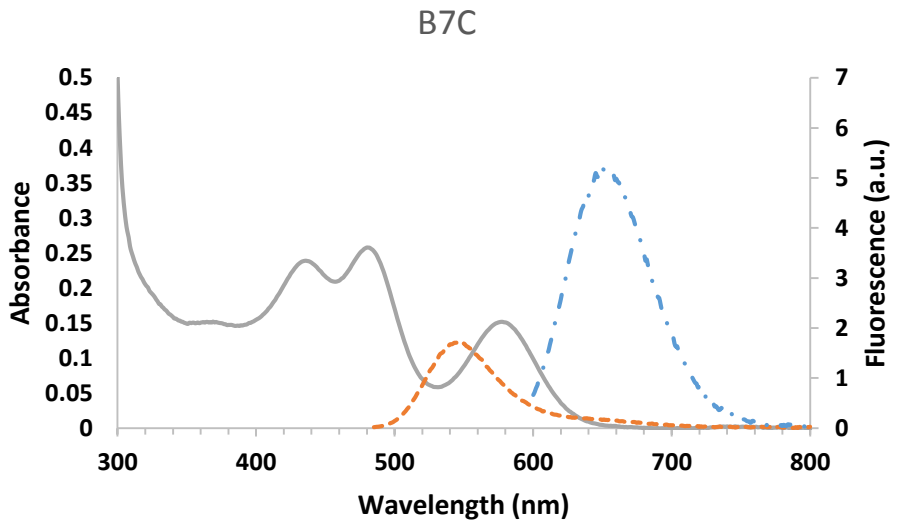

Figure 5. Absorbance and fluorescence spectra at excitation wavelengths of 465nm and 580nm from B7C AgNCs at 2 hours after synthesis

The grey solid line corresponds to the absorbance spectrum and the orange dashed and blue alternating lines correspond to fluorescence spectra at excitation wavelengths of 465nm and 580nm, respectively.

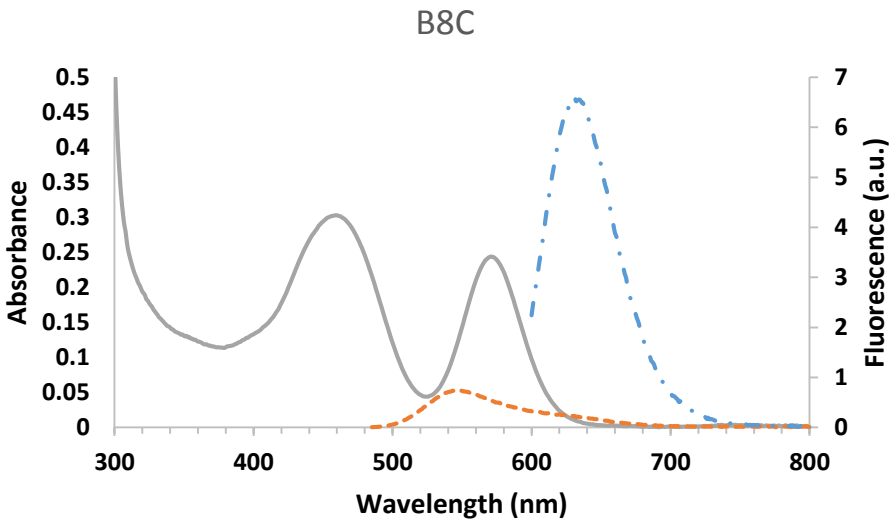

Figure 6. Absorbance and fluorescence spectra at excitation wavelengths of 465nm and 580nm from B8C AgNCs at 2 hours after synthesis

The grey solid line corresponds to the absorbance spectrum and the orange dashed and blue alternating lines correspond to fluorescence spectra at excitation wavelengths of 465nm and 580nm, respectively.

B8C formed a smaller number of discrete absorbing populations at higher optical densities relative to the other bubbles with maximum absorbance values of 0.303 and 0.244 at 459nm and 571nm, respectively. B5C gave maxima of 0.202, 0.173, and 0.136 at 393nm, 432nm, and 495nm, respectively. B7C formed species more similar to B8C with maxima of 0.151, 0.239, 0.258, and 0.152 at 373nm, 436nm, 480nm, and 577nm, respectively. These BnC AgNCs also appear to have a trace population absorbing near 350nm that is largely obscured by the intense absorbance of DNA that begins at 350 nm and reaches a maximum at 280 nm. Spectra of BnC AgNCs with *n*=2, 3, 4, 6, 10, 12, and 16 are not shown because they resulted in much lower yields and less intensely fluorescing species than clusters with *n* = 5,7and 8. B5C AgNCs emit at 568nm and 631nm with intensities of 1.174 and 0.990. Emissions of 1.707 and 5.241 at 545nm and 649nm and emissions of 0.747 and 6.605 at 545nm and 631nm were observed for B7C and B8C AgNCs, respectively. These green and red emitting species are reminiscent of ssDNA-AgNCs synthesized in many published accounts. [7,8]

Absorbance spectra from figures 4, 5, and 6 have been overlaid with their respective fluorescence excitation spectra in figures 7, 8, and 9. The excitation spectra were obtained by exciting BnC AgNC samples from 250nm to 600nm and observing fluorescence at 620nm. The excitation spectra are simply normalized to 0.5 for the sake of comparison with the absorbance spectra. For B5C AgNCs, populations absorbing about 565nm, 506nm, 370nm, and 300nm are shown in the excitation spectrum. 300nm and 506nm excitations correlate with strong absorbance peaks. A small peak near 565nm may be present in the absorbance spectrum, which could account for the long slope of the 495nm absorbing population. The 370nm excitation may also correlate with a weak absorbance of the AgNCs between the absorbances of DNA. Higher energy electronic transistions corresponding to shorter wavelengths at 370nm and 300nm in the

excitation spectrum are seen contributing to fluorescence at 620nm, with the 300nm excitation nearing the intensity of those at 565nm and 506nm.

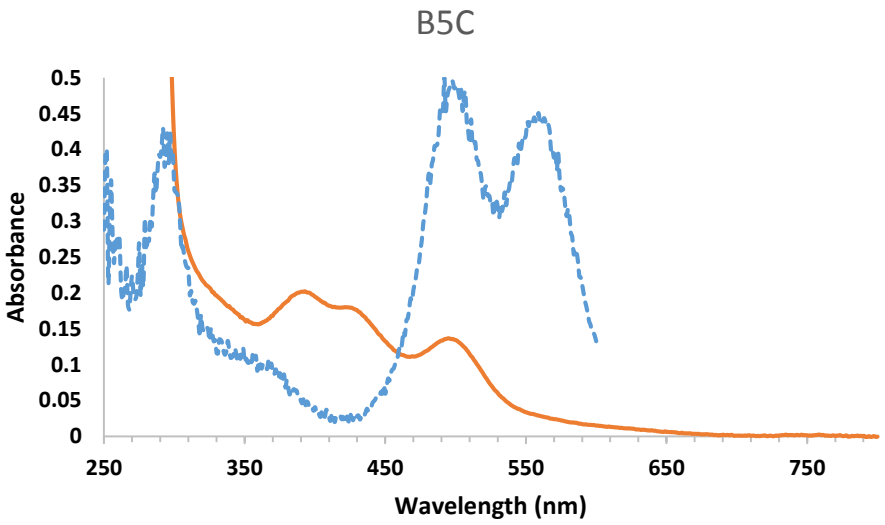

Figure 7. Normalized 620nm fluorescence excitation (blue dashed line) and absorbance (orange solid line) spectra of B5C AgNCs

B7C and B8C AgNCs show very similar excitation profiles to B5C AgNCs for 620nm fluoescence, except the relative intensities of the 582nm (B7C) and 576mn (B8C) excitation wavelengths dominate these spectra. Distinct excitation wavelengths can still be observed about 300nm with less intense peaks about 370nm.

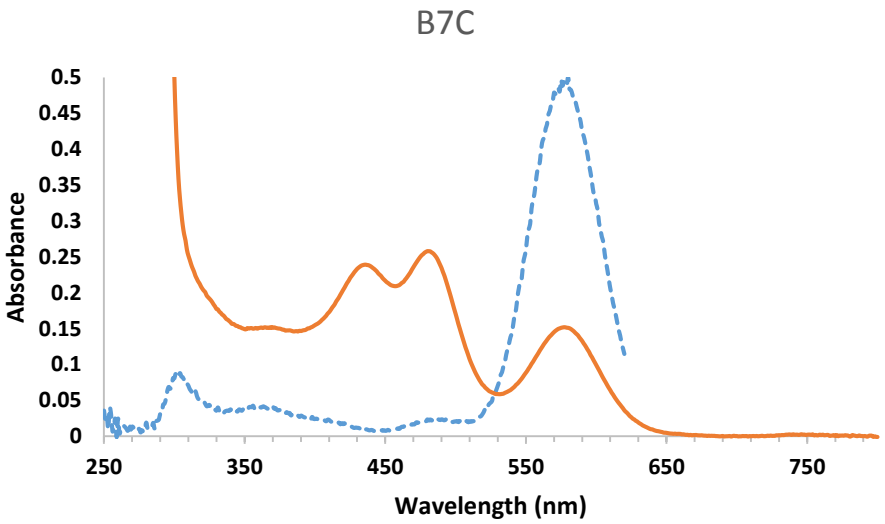

Figure 8. Normalized 620nm fluorescence excitation (blue dashed line) and absorbance (orange solid line) spetra of B7C AgNCs

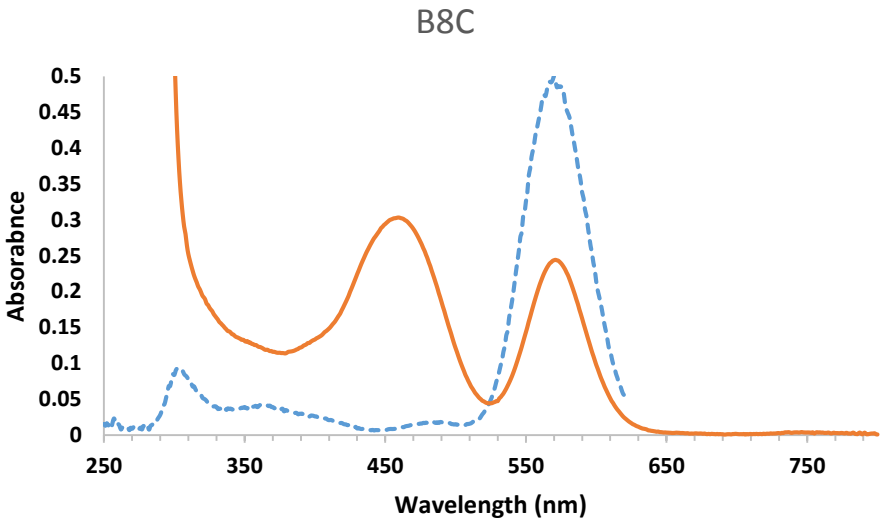

Figure 9. Normalized 620nm fluorescence excitation (blue dashed line) and absorbance (orange solid line) spectra of B8C AgNCs

Figure 10 shows fluorescence spectra obtained by exciting populations absorbing at much higher energies than the major absorption peaks at 480 and 577 nm (Figure 6). Note the appearance of only two emission peaks despite exciting populations that absorb more than

300nm from the emission wavelength. Also, the relative intensities of these emission spectra correspond with the relative intensities of these populations in the excitation spectra, which is to be expected.

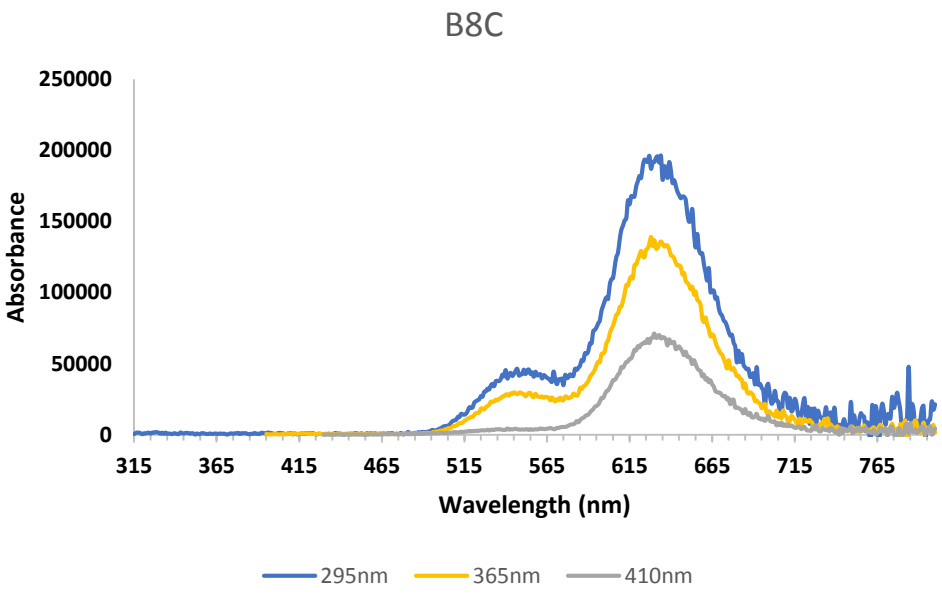

Figure 10. Fluorescence from B8C AgNCs when excited at 295, 365, and 410nm

Time-dependent fluorescence spectra were recorded for B5C, B7C, and B8C AgNCs. The fluorescence maxima were plotted as functions of time in Figures 11, 12, and 13. BC5 AgNCs emitting at 565nm reach their minimum emission at approximately 30 hours while 630nm emitters decay to 20% of their maximum intensity after 80 hours. B7C AgNCs emitting at 650nm are of roughly the same stability as the analogous B5C species, however, the B7C 545nm emission showed a large increase in stability over the analogous population for B5C AgNCs. The 545nm fluorescence from B7C decayed to 80% of its maximum value after 116 hours. B8C AgNCs yielded the most stable fluorescent species with the 630nm emission decaying to 16% of its maximum value after 116 hours. The most stable population formed in

this experiment was the B8C species emitting at 550nm, which continued to increase in fluorescence intensity over the course of 116 hours.

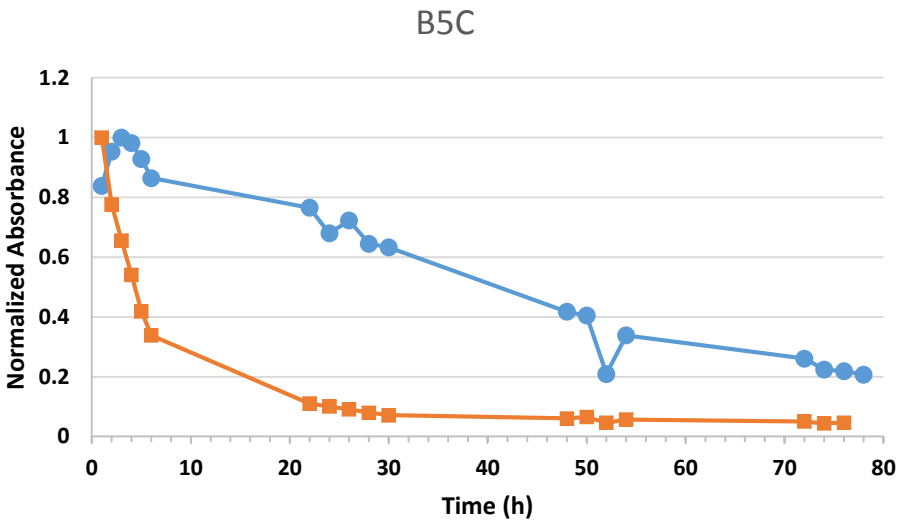

Figure 11. Graphical representation of fluorescence intensities of B5C AgNCs 565nm (blue circles) and 630nm (orange squares) emitting populations are shown decaying with time.

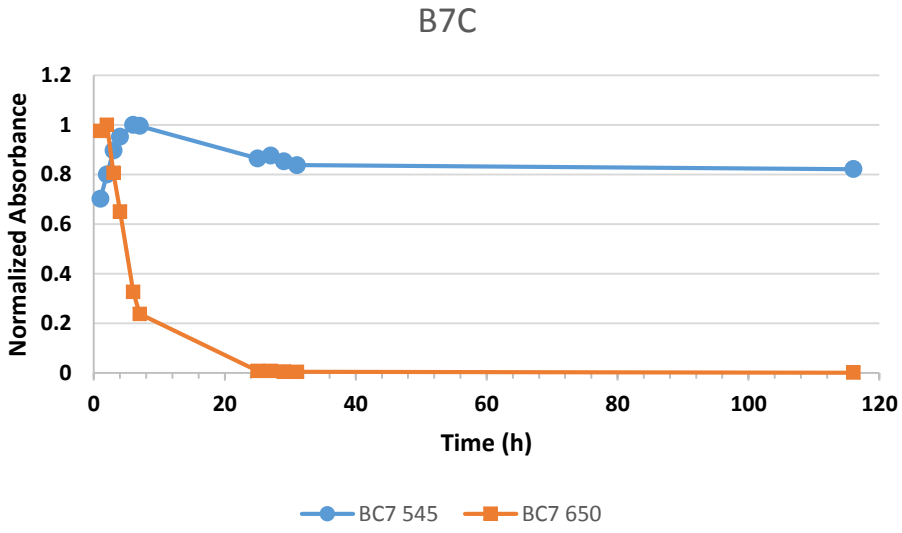

Figure 12. Graphical representation of fluorescence intensities of B8C AgNCs 545nm (blue circles) and 630nm (orange squares) emitting populations are shown decaying with time.

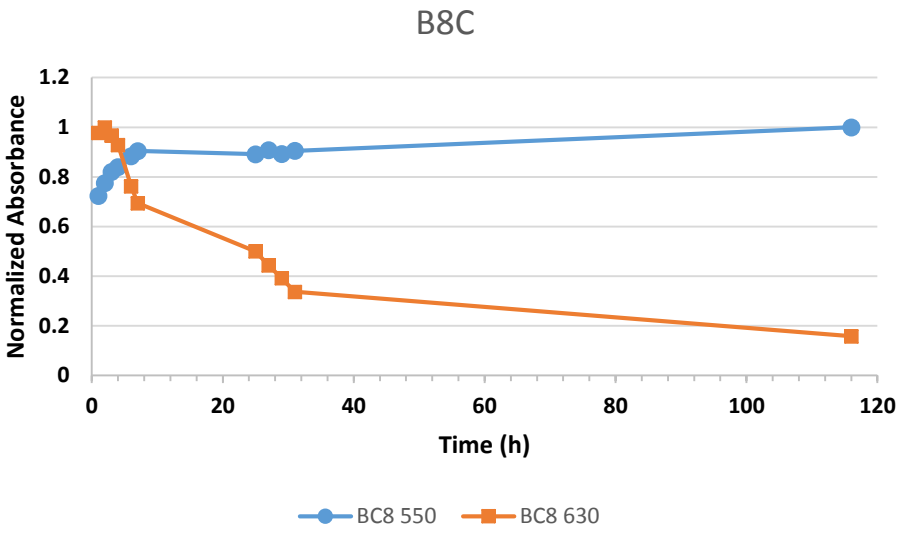

Figure 13. Graphical representation of fluorescence intensities of B8C AgNCs

550nm (blue circles) and 630nm (orange squares) emitting populations are shown decaying with time.

3.2 Optimizing Silver-to-Sodium Borohydride-to-DNA Ratio for B8C AgNCs

Silver-to-sodium borohydride-to-DNA (Ag:$NaBH_4$:DNA) ratios ranging from 1:1:1 to 6:6:1 yielded no measurable fluorescence. Ratios of 8:8:1, 10:10:1, 14:14:1, 16:16:1, 18:18:1, and 24:24:1 gave fluorescence intensities centered around a roughly maximized value of 14:14:1. The range of Ag:DNA ratios chosen for the Box-Behnken experimental design was based on this maximum.

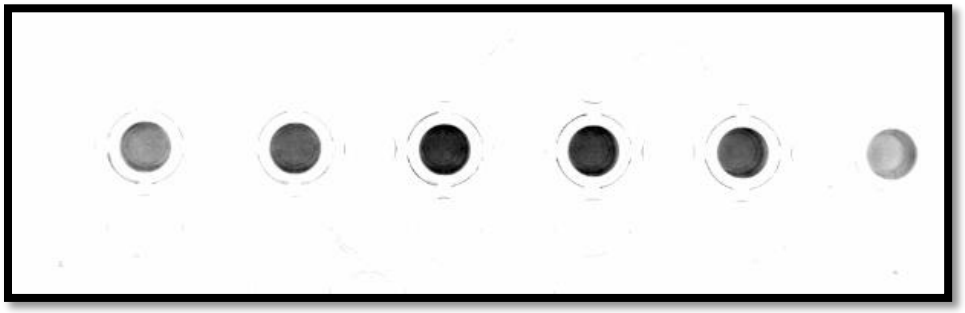

Figure 14. High-contrast greyscale image of fluorescing B8C AgNCs made at different Ag:$NaBH_4$:DNA

Ag:$NaBH_4$:DNA of 8:8:1, 10:10:1, 14:14:1, 16:16:1, 18:18:1, and 24:24:1 are shown left to right in alternating wells of a 96-well microtitre plate. Darker areas indicate more intense fluorescence. The image was taken under UV illumination by a Kodak Image Station 4000R Pro and was manipulated in Carestream Imaging Software.

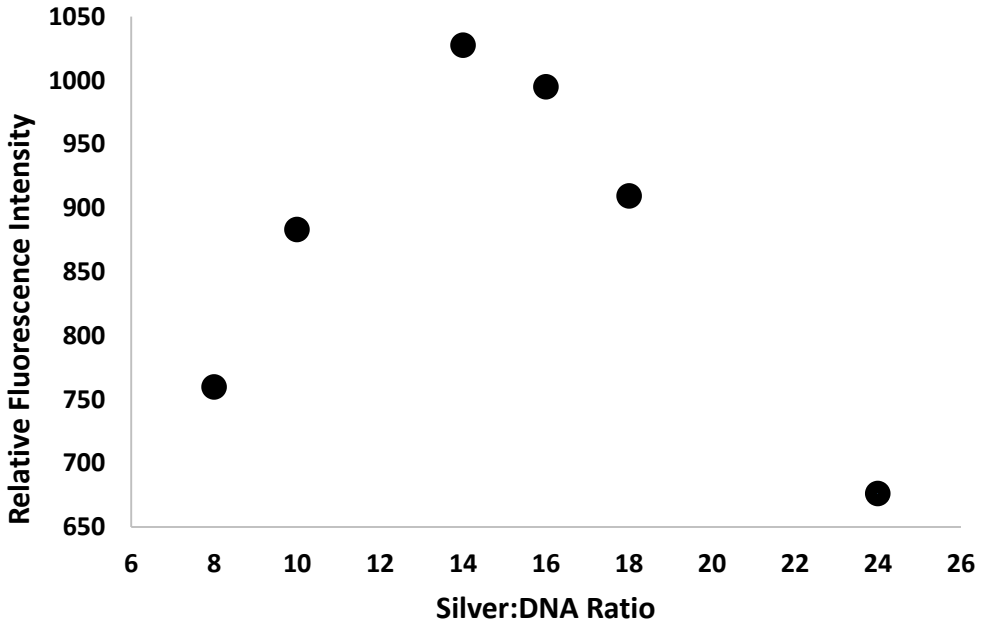

Figure 15. Graphical representation of B8C fluorescence intensities at various Ag:$NaBH_4$:DNA

Note the maximum at Ag:$NaBH_4$:DNA=14. This figure was obtained by graphing values assigned to each well by the pixel counting function of Carestream Imaging Software applied to the images in Figure 14.

3.3 Comparing Single and Hybridized B8C Bubble DNA Sequences

Figures 16 and 17 show the time-dependence of the peak fluorescence intensities from AgNC templated using non-hybridized Bottom and Top ssDNA strands used to make B8C, respectively. These AgNCs were less stable than those formed on the hybridized B8C template with respect to each population. Both Bottom and Top AgNCs formed a 630nm emitting species

that decayed to near 0% of its original fluorescence after 48 hours. Bottom AgNCs reached maximum fluorescence around one day after synthesis and began to decay thereafter, reaching 75% of the maximum fluorescence in 24 hours. Top AgNCs reached maximum fluorescence in a few hours after synthesis and decayed to 85% of the maximum fluorescence after roughly 48 hours.

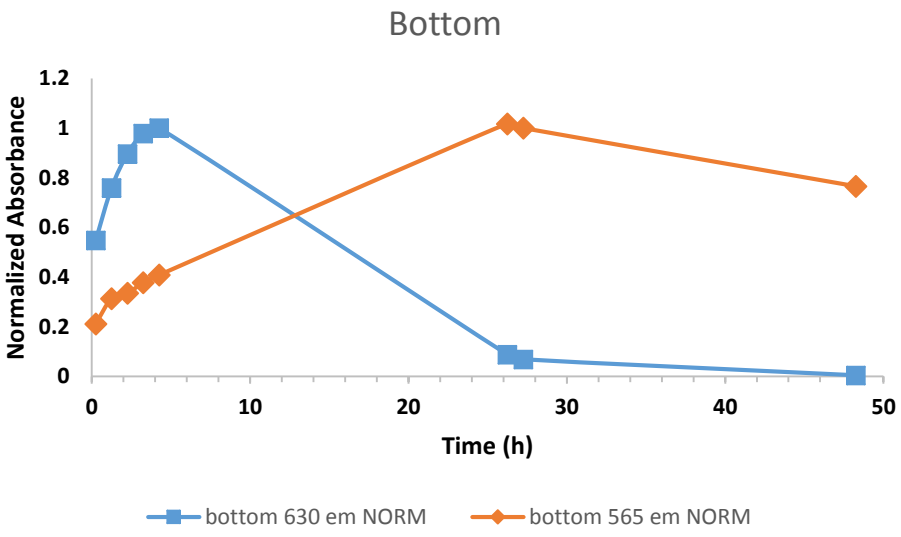

Figure 16. Fluorescence intensities of B8C Bottom AgNCs at 565nm and 630nm versus time

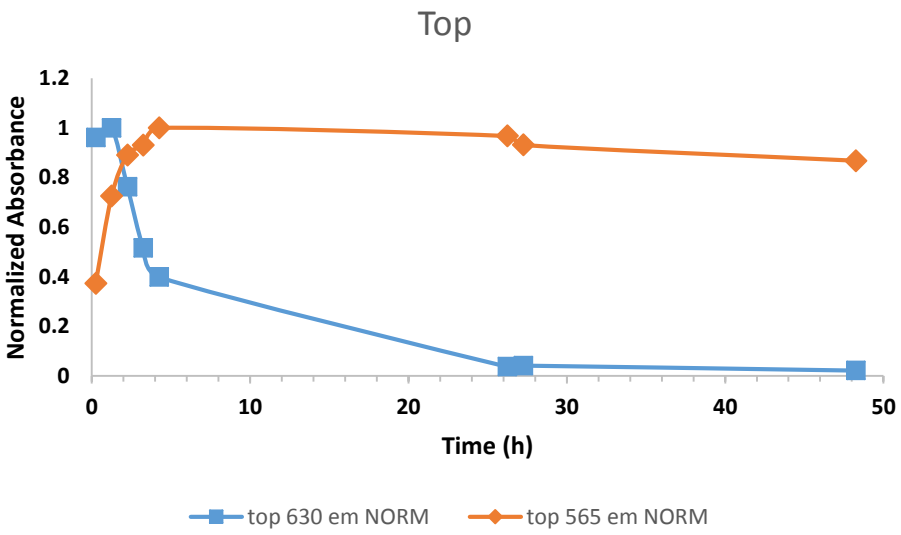

Figure 17. Fluorescence intensities of B8C Top AgNCs at 565nm and 630nm versus time

3.4 Synthesis Optimization Via a Box-Behnken Experimental Design

While performing the Box-Behnken experimental design [6], one obvious trend was noticed. Solutions containing no buffer formed an orange solution while buffered samples became pink (Figure 18). The pink solutions eventually turned orange as their fluorescence and absorbance decreased in intensity and all orange solutions faded to yellow upon further degradation. Thus, pink coloration and the presence of phosphate buffer correspond to a sample with more stable fluorescing and absorbing populations.

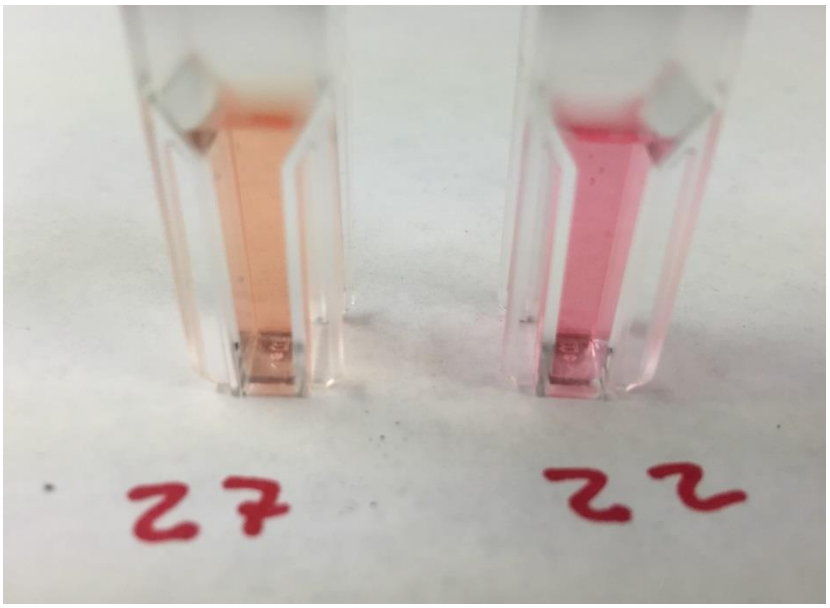

Figure 18. Box-Behnken samples 27 (left) and 22 (right).

These samples show the effect of phosphate buffer on otherwise identical solutions of B8C AgNCs. The orange solution (left) contains no buffer, while the pink solution (right) contains 10μM phosphate buffer.

Figure 19 shows response optimization of "Stable" and "Yield", which correspond to the reciprocal of each sample's decay rate and each sample's maximum absorbance, respectively.

The decay rates for chemical yield were calculated by fitting each population's maximum absorbance values versus time with the equation:

$$\ln[A] = \ln[A]_0 - kt \quad (1)$$

where $[A]_0$ is the initial absorbance and [A] is the maximum absorbance of a sample at time *t*, measured in hours. The rate constant *k*, measured in hours^{-1}, is a measurement of how quickly [A] decays as a function of time. The reciprocal of the decay rates, or lifetimes, correspond directly with B8C AgNC stability (larger 1/*k* means greater stability) and maximum absorbance values correspond with the maximum chemical yield.

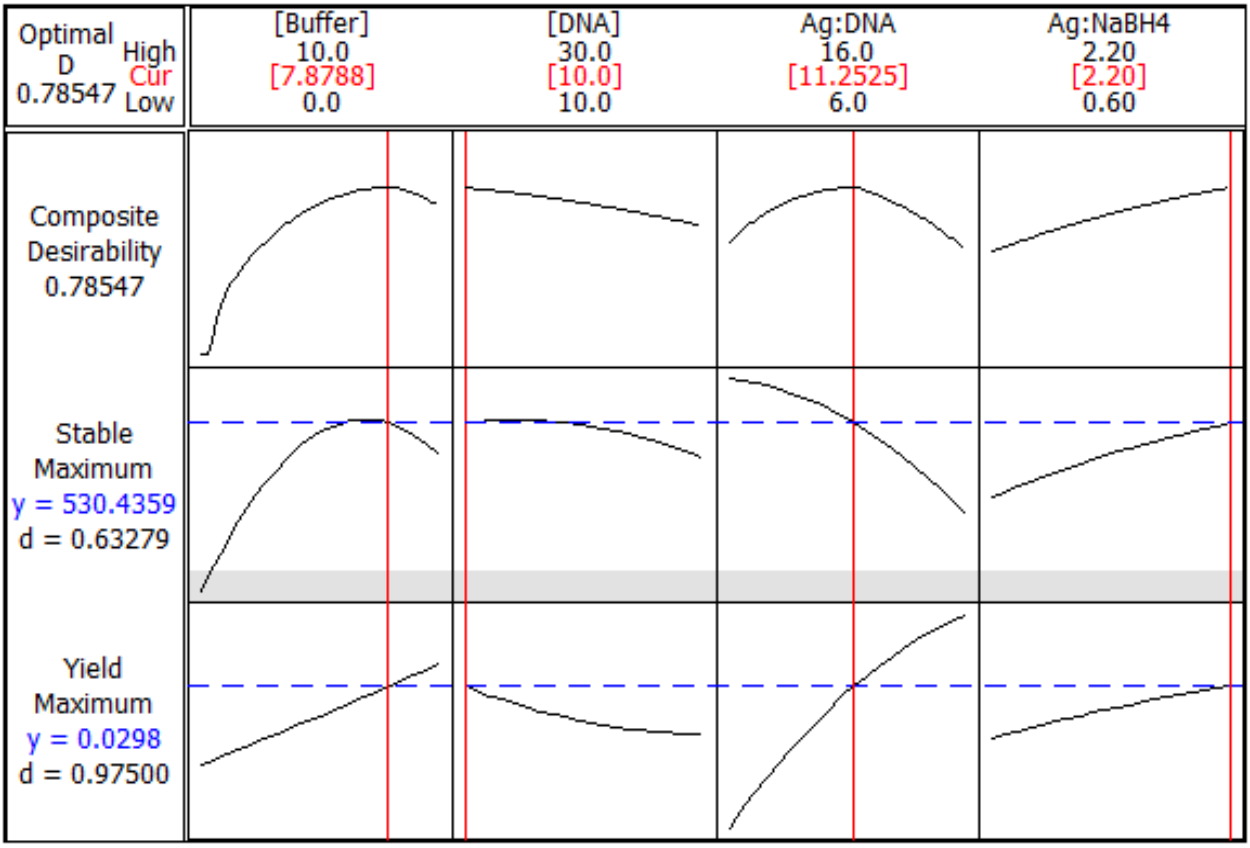

Figure 19. An array of plots created by processing Box-Behnken experimental design data via Minitab™ software

Labels along the top indicate which column corresponds to the optimization of which control factor. Optimized control factor values (y values) are shown as red vertical lines. The composite desirability of each control factor (d value) is indicated by a horizontal, blue, dashed line.

B8C AgNCs have maximum stability at ~7μM buffer concentration. Stability decreases with increasing DNA concentration and silver-to-DNA ratio, possibly by a logarithmic dependence. Stability increases at higher silver-to-sodium borohydride ratios. Chemical yield increases with buffer concentration, silver-to-DNA ratio, and silver-to-sodium borohydride ratio, but decreases with increasing DNA concentration. These trends were combined by the response optimizing function in Minitab^{TM} to give the top row, "Composite Desirability", which calculates ideal control factor values for the simultaneous optimization of the stability and chemical yield response factors. Optimal buffer concentration, DNA concentration, silver-to-DNA ratio, and silver-to-sodium borohydride ratio were found to be 7.88μM, 10.0μM, 11.25, and 2.20, respectively.

Values of 0.785, 0.633, and 0.975 mark quantified, internal composite desirability of the combined, stability, and chemical yield columns. A value close to one indicates optimal composite desirability, meaning that the dependences of a response factor upon each control factor are in close agreement with respect to the optimized control factor value. Therefore, the various dependences of chemical yield are in high agreement with one another, with combined and stability response factors following. The y values indicate the largest possible maximum obtainable by a response factor with respect to varying each of its control factors.

Chapter 4

Discussion

4.1 Optimizing *n* in B*n*C Bubble DNA Templates

B*n*C templates with *n*=2, 3, 4, 6, 9, 10, 12, and 16 made much less stable AgNCs compared to B5C, B7C, and B8C. B5C, B7C, and B8C AgNCs have some very similar absorbing populations at similar wavelengths in different ratios. Analogous absorbance and emission bands are grouped horizontally in Table 1.

Table 1 Wavelengths (nm) of absorbance and fluorescence bands as seen in Figures 4, 5, and 6. The wavelengths are grouped according to similarity

Absorbance maxima (nm)			Fluorescence maxima (nm)		
B5C	B7C	B8C	B5C	B7C	B8C
350	350	350	-	-	-
393	373	-	-	-	-
432	436	-	-	-	-
495	480	459	568	545	545
-	577	571	631	649	631

As *n* increases, absorbing populations appear at longer wavelengths, which is seen especially between B5C to B8C AgNCs. B8C AgNCs even fail to form some shorter wavelength populations seen in B5C, indicating that the bubble templates favor different species. The 459nm band formed by B8C AgNCs, however, is much broader than the one at 571nm and may be a combination of a fluorescing and non-fluorescing species as well as the low optical density of DNA in this region.

The formation of different AgNC species may be described by a model by Schultz et. al. wherein discrete DNA-AgNC sizes were characterized by the number of silver atoms in a single

DNA template via mass spectrometry. [7] It is possible that B*n*C templates of varying *n* create nanoclusters consisting of different numbers of silver atoms that absorb and fluoresce at different energies or absorb without fluorescing. Non-fluorescent species could account for absorption bands at 436nm and below that have no corresponding fluorescence.

Fluorescence excitation scans of B5C, B7C, and B8C AgNCs show absorbance bands near 300nm and 370nm giving excitation spectra characteristic to many organic dyes. Thus UV absorbance bands are most likely electronic transitions within AgNCs that give the more intense lower energy emissions. Interestingly, the excitation spectrum of B5C AgNCs shows an absorbance band about 565nm, which is not seen in the absorbance spectrum. This population is most likely present in the long curve tailing from the absorbance band at 495nm. The increasing relative intensity of the absorbance band at ~570nm from Figures 7 to 9 is also evidence for the notion that varying *n* in B*n*C templates stabilizes different AgNCs.

Figure 10 shows that no absorbing species fluoresce at wavelengths other than ~550nm and ~630nm. The contribution of the ~300nm absorbing species to fluorescence is greater than that from AgNCs absorbing at ~370, which correlates with the peaks seen on the fluorescence excitation scans in Figures 7-9.

Figures 11-13 give the final rationale for choosing to optimize B8C AgNCs over other *n* B*n*C AgNCs. LSC materials must be strong and stable emitters. While B7C AgNCs give the most intense green emission, B8C AgNCs give the strongest red emission and are the most stable. It is possible that 550nm emission of B8C AgNCs reached a maximum between 31 and 116 hours, making them less stable than they appear, however an increase in fluorescence was still observed from 31 to 116 hours, which is unique to this population.

4.2 Optimizing Silver-to-Sodium Borohydride-to-DNA Ratio for B8C AgNCs

B4C and B12C AgNCs were treated as seen in Figures 14 and 15; however, only the B8C template yielded nanoclusters bright enough to image. B4C and B12C AgNCs gave weak fluorescence for less than half the total time of observable B8C AgNCs, which also suffered significantly decreased longevity while in microwell plates compared to decay rates given in Figures 11-13. Even B8C solutions reacted at Ag:DNA below 8:8:1 failed to form nanoclusters bright enough for imaging. These decreases in stability have been attributed to lesser photostability on the part of B4C and B12C AgNCs and dissolved oxygen, as the microwell samples had much greater surface area than the cuvette samples which could facilitate the dissolving of gases. Other laboratories have documented oxygen as being detrimental to DNA-AgNC stability. [9]

Increasing the concentration of $NaBH_4$ was also a concern since it may have basified the solution by forming $NaBO_2$ as a product from the decomposition of water. Basifying or acidifying DNA solution too far beyond physiological pH interferes with hydrogen bonding that gives rise to α-helix dsDNA, which could affect the stability and formation of B*n*C AgNCs. High concentrations of $NaBH_4$ may also be able to reduce functional groups like amides.

4.3 Comparing Single and Hybridized B8C Bubble DNA Sequences

Figures 16 and 17 clearly communicate that AgNCs synthesized using unhybridized DNA templates are much less stable than those made on the associated dsDNA B8C template. Approximately one day after synthesis, the red emissions of Bottom and Top ssDNA templates decayed to less than 10% their maximum observed fluorescence values, while the dsDNA B8C

template had decayed to roughly half its maximum in the same amount of time. This increase in stability is attributed to greater protection of the AgNC by the dsDNA template. The hairpin is the most widely accepted form of ssDNA templates for AgNCs. A hairpin would theoretically provide as much protection as a dsDNA bubble; however, hairpins are much more strained by bending around the AgNC, which does not need to be achieved by the bubble DNA template. Thus, hairpins likely dissociate more than bubble templates due to physical strain and less base pairing per template, providing less protection for AgNCs from aggregation and oxidation.

4.4 Synthesis Optimization Via a Box-Behnken Experimental Design

The pink coloration of buffered samples is due to the stabilization of the population absorbing about 571nm. As this population decays, it transmits more yellow and orange light and the solution appears to fade to orange then to yellow in color. This change can be used to quantitatively assess the stability of B8C AgNCs, a phenomenon that could be used to assess the performance of LSCs impregnated with B8C AgNCs.

For photostability and chemical yield analyses, absorbance spectra were taken of the 630nm emitter of B8C AgNCs. The 545nm emitter was not observed because other non-fluorescing species complicated the decay pattern. It is also hypothesized that 630nm emitters change into 545nm emitters as they decay, further complicating the properties of the 545nm emitters. 630nm emitters, on the other hand, appear to decay based on first-order kinetics, which were used to determine the rates of decay for each sample.

Increasing buffer concentration gives a near linear increase in chemical yield and a second-order maximum about 7μM for photostability. The composite desirability of these

functions considers that the increase in chemical yield is eventually outweighed by the decrease in photostability. Both photostability and chemical yield decrease as DNA concentration increases, which gives an optimal DNA concentration of 10μM. This maximum is erroneously assigned as it is the limit of this axis in the experimental design. An optimal DNA concentration probably exists at concentrations lower than 10μM. Increases in stability chemical yield attributed to low DNA concentration are likely due to the lack of AgNC aggregation in dilute solutions. Such aggregation would quench AgNC fluorescence.

Photostability and chemical yield show inverse and direct correlation, respectively, with Ag:DNA. Here, the composite desirability function considers both trends at an intermediate point where neither photostability nor chemical yield suffers greatly. Increasing Ag:$NaBH_4$ gives rise to a situation similar to manipulating DNA concentration. Photostability and chemical yield have nearly identical dependencies upon Ag:$NaBH_4$ such that the ideal ratio of 2.20:1 is probably an overestimate. Other research groups have documented DNA-AgNC syntheses using Ag:$NaBH_4$ ratios of 2:1 and 1:1 [7], but our experimental design indicates that even lower ratios maybe optimal for the bubble DNA templates. This low concentration of $NaBH_4$ also supports the earlier hypothesis that increasing $NaBH_4$ concentration was detrimental to the formation of AgNCs in the microwell experiment. More experimentation will be carried out to determine the true limits of the unoptimized factors in this design. Also data that will be used to characterize the dependency of fluorescence quantum yield on these control factors has been recorded and will be processed.

Chapter 5

Conclusion

Bubble DNA-AgNCs were successfully synthesized, by hybridizing the strands 5'-CTGACTCCC*n*TGGGAGAA -3' and 5'- TTCTCCCAC*n*GGAGTCAG -3' with *n*=2, 3, 4, 5, 6, 7, 8, 10, 12, and 16 cytosine pairs. Two distinct fluorescent populations emitting at ~545nm and ~630nm and absorbing at ~470nm and ~570nm, respectively, were formed from each bubble template, although some bands were not present in all spectra as seen with B5C AgNCs. The bubble template with 8 cytosine pairs formed the most stable AgNCs and the brightest ~630nm emitter, while the 7 cytosine pair template formed the brightest ~545nm emitter. Preliminary optimized Ag:$NaBH_4$:DNA was found to be 14:14:1. Single stranded bubble templates were found to be much less stable than hybridized bubble templates. Finally, optimal phosphate buffer (pH=7) concentration, DNA concentration, silver-to-DNA ratio, and silver-to-sodium borohydride ratio were found to be 7.88μM, 10μM, 11.25, and 2.20, respectively, via Box-Behnken experimental design with chemical yield and photostability as response factors.

Appendix A

Parameters Used for Box-Behnken Analysis

Experiment Number	[Buffer] (μM)	[DNA] (μM)	Ag:DNA	Ag:$NaBH_4$
1	5	20	11	1.4
2	10	20	16	1.4
3	5	30	11	2.2
4	5	30	11	0.6
5	0	20	6	1.4
6	5	10	11	2.2
7	10	20	6	1.4
8	0	20	16	1.4
9	5	10	11	0.6
10	5	30	6	1.4
11	5	10	16	1.4
12	0	20	11	2.2
13	5	10	6	1.4
14	0	20	11	0.6
15	5	30	16	1.4
16	10	20	11	2.2
17	10	20	11	0.6
18	5	20	11	1.4
19	5	20	16	0.6
20	5	20	16	2.2
21	0	10	11	1.4
22	10	30	11	1.4
23	5	20	6	0.6
24	5	20	11	1.4
25	10	10	11	1.4
26	5	20	6	2.2
27	0	30	11	1.4

BIBLIOGRAPHY

[1] J.S. Batchelder, A.H. Zewail and T. Cole, Luminescent Solar Concentrators. 1: Theory of Operation and Techniques for Performance Evaluation, Applied Optics, 1979, 18, 3090-3110.

[2] E. Braun, Y. Eichen, U. Sivan and G. Ben-Yoseph, DNA-Templated Assembly and Electrode Attachment of a Conducting Silver Wire, Nature, 1998, 391, 775-778.

[3] Sharma, J.; Rocha, R. C.; Phipps, M. L.; Yeh, H.-C.; Balatsky, K. A.; Vu, D. M.; Shreve, A. P.; Werner, J. H.; Martinez, J. S. A DNA-Templated Fluorescent Silver Nanocluster with Enhanced Stability. *Nanoscale*. **2012**, *4*, 4107.

[4] Orbach, R.; Guo, W.; Wang, F.; Lioubashevski, O.; Willner, I. Self-Assembly Of Luminescent Ag Nanocluster-Functionalized Nanowires. *Langmuir*. **2013**, *29*, 13066–13071.

[5] Box, G. E. P.; Wilson, K. B. On the Experimental Attainment of Optimum Conditions. *J. R. Stat. Soc.* **1951**, *13*, 1-45.

[6] 5.3.3.6.2. Box-Behnken designs. 5.3.3.6.2. Box-Behnken designs, http://www.itl.nist.gov/div898/handbook/pri/section3/pri3362.htm (accessed Apr 11, 2016).

[7] Schultz, D.; Gardner, K.; Oemrawsingh, S. S. R.; Markešević, N.; Olsson, K.; Debord, M.; Bouwmeester, D.; Gwinn, E. Evidence For Rod-Shaped DNA-Stabilized Silver Nanocluster Emitters. *Adv. Mater. Advanced Materials*. **2013**, *25*, 2797–2803.

[8] Han, B.; Wang, E. DNA-Templated Fluorescent Silver Nanoclusters. *Anal Bioanal Chem Analytical and Bioanalytical Chemistry*. **2011**, *402*, 129–138.

[9] Volkov, I. L.; Ramazanov, R. R.; Ubyivovk, E. V.; Rolich, V. I.; Kononov, A. I.; Kasyanenko, N. A. Fluorescent Silver Nanoclusters In Condensed DNA. *ChemPhysChem*. **2013**, *14*, 3543–3550.

ACADEMIC VITA

Academic Vita of Ian Campbell
iec5014@psu.edu

Education

Penn State Erie, The Behrend College, Schreyer Honors College

- Bachelor of Science in Chemistry, Minor in Physics — *anticipated 2016*
- Dean's List all semesters — *Fall 2012-present*

Semester abroad at University College Dublin — *Fall 2015*

Harbor Creek High School, Harborcreek PA — *2012*

Work Experience

Undergraduate Research at Penn State Behrend

- Optimization of the preparation of nanoclusters as luminescent solar concentrator (LSC) materials – Supervisor: Dr. Bruce Wittmershaus — *June 2014-present*
- Infrared analysis of transient species trapped in inert matrices via infrared matrix isolation spectroscopy – Supervisor: Dr. Jay Amicangelo — *June 2013-May 2014*

Undergraduate Research at University College Dublin — *Fall 2015*

- Optimized qualities of a nanotechnology-based assay using superparamagnetic beads and specific biological reactions to detect cardiac troponin and exosomes - Supervisor: Dr. Gil Lee

Teaching assistant for Electricity and Magnetism at Penn State Behrend — *Spring 2014*

- Assisted students with in-class activities and graded classwork

Technical Experience

Fluorescence, UV-vis absorption, Infrared, and NMR spectroscopies
Column, gas, and high performance liquid chromatographies
Extractions, titrations, chemical syntheses within isolated atmospheres, qualitative analyses, small volume syntheses, ELISA

Leadership & Community Service

Teaching assistant for Electricity and Magnetism at Penn State Behrend — *Fall 2014*

Study session leader for Electricity and Magnetism at Penn State Behrend — *Fall 2014*

- Taught/reviewed concepts with up to 40 students during extracurricular study sessions

Volunteer at National Chemistry Week demonstration — *Nov 2014*

Grants & Awards

Northwest Pennsylvania Chapter of Sigma XI and Penn State Behrend Undergraduate Research Conference — *2015 & 2014*

- First place and runner-up

Erickson Discovery Grant *Summer 2015*

- Highly competitive University-wide grant at Penn State

Herbert Award Summer Grant *2015*

Joseph A. and Berit I. Bennaci Family Scholarship *2012-2013, 2013-2014*

Presentations

Northwest Pennsylvania Chapter of Sigma XI and Penn State Behrend Undergraduate Research Conference

- Oral: "Temperature Dependence of the O–H Stretching Peak of the Methanol-Benzene Complex in an Argon Matrix" *2014*
- Oral: "Optimization of Fluorescence Intensity and Stability of 'Bubble' DNA Templated Silver Nanoclusters" *2015*

National Council on Undergraduate Research *2015*

- Poster: "Characterization of 'Bubble' DNA Templated Silver Nanoclusters as a Fluorescent Material"